A new car-following model yielding log-normal type headways distributions*

Li Li(李 力)[a)†], Wang Fa(王 法)[a)], Jiang Rui(姜 锐)[b)], Hu Jian-Ming(胡坚明)[a)], and Ji Yan(吉 岩)[a)]

[a)] *Tsinghua National Laboratory for Information Science and Technology (TNList), Department of Automation, Tsinghua University, Beijing* 100084, *China*

[b)] *School of Engineering Science, University of Science and Technology of China, Hefei* 230026, *China*

(Received 1 October 2008; revised manuscript received 8 April 2009)

Modeling time headways between vehicles has attracted increasing interest in the traffic flow research field recently, because the corresponding statistics help to reveal the intrinsic interactions governing the vehicle dynamics. However, most previous micro-simulation models cannot yield the observed log-normal distributed headways. This paper designs a new car-following model inspired by the Galton board to reproduce the observed time-headway distributions as well as the complex traffic phenomena. The consistency between the empirical data and the simulation results indicates that this new car-following model provides a reasonable description of the car-following behaviours.

Keywords: traffic flow, car-following, log-normal distribution

PACC: 0550, 0520

1. Introduction

To explain and reproduce the complex phenomena of road traffic, the dynamics of traffic flows are often described on N strongly-coupled particles (vehicles) under fluctuations.[1] Since the governing interaction forces or potentials between these particles cannot be directly measured, the statistical features of particles are often investigated instead.[2]

Among different statistical features, the distributions of space-gaps/time-headways between these particles (vehicles) received consistent interest. In some recent studies,[3−6] some theoretical models were presented from different physical perspectives (e.g. scatter theory and random matrix theory (RMT)) to explain why the observed time-headway distributions have similar shapes even for different phases (i.e. Kerner's three divisions: free flows, synchronized flows, and moving jams[2]). For example, in Ref. [5], the following probability density function $f(s)$ is chosen to model the practical distributions based on random-matrix theory

$$f(\alpha, s) = \frac{16}{\pi^2 D_0 \mathrm{K}_1(2\alpha)} s^2 \times \int_0^\infty \exp\left[-\alpha\left(\frac{D}{D_0}+\frac{D_0}{D}\right)-\frac{4s^2}{\pi D^2}\right]\frac{\mathrm{d}D}{D^3}, \quad (1)$$

where α and D are two shape controlling coefficients determined by the sampling data. D_0 is then chosen as $D_0 = \mathrm{K}_1(2\alpha)/\mathrm{K}_2(2\alpha)$ and $\mathrm{K}_m(x)$ is a modified Bessel function of the second kind.

In some recent reports, the practical headways are assumed to follow certain log-normal distributions.[7,8]

$$f(s) = \frac{1}{\sigma\sqrt{2\pi}h}\,\mathrm{e}^{(\ln s-\mu)^2/2\sigma^2}, \quad (2)$$

where μ and σ denote the mean and variance of the sampling data.

Figure 1 shows the comparison results for the empirical, super-statistical[5] and log-normal distributions $P(\tau)$, where $\tau = t_\mathrm{h}/\langle t_\mathrm{h}\rangle$, t_h denotes the sampled time-headways and $\langle t_\mathrm{h}\rangle$ is its mean value. It is clear that log-normal distribution model has smaller fitting errors.

However, how these log-normal distributions are generated remained to be studied previously. In this paper, we propose a new car-following model inspired by the Galton board to explain this interesting phenomena.

*Project supported partly by the National Basic Research Program of China (Grant No. 2006CB705506), the National Hi-Tech Research and Development Program of China (Grant Nos. 2006AA11Z215 and 2007AA11Z222), and the National Natural Science Foundation of China (Grant Nos. 50708055, 60774034 and 10872194).

†Corresponding author. E-mail: li-li@mail.tsinghua.edu.cn

© 2010 Chinese Physical Society and IOP Publishing Ltd

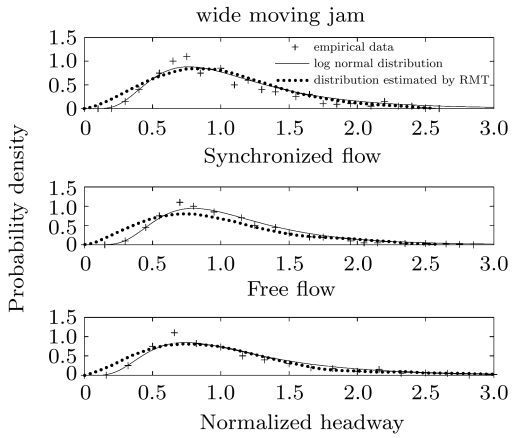


Fig. 1. Probability density $P(\tau)$ for normalized empirical time-headways τ between successive cars in traffic flow. For comparison, the empirical data and super-statistical distributions on RMT are excerpted from Ref. [5].

2. The car-following model inspired by Galton board

2.1. The idea behind

Before we present the main model, let us interpret the stochastic process yielding log-normal type distributions using the generative model method. As pointed out by Galton 1889 in Ref. [9], the dynamics of such stochastic processes can be modeled as a particle falling down a board (such a board is called Galton board) and being deviated at decision points (the tips of the triangular obstacles) either left or right, see Fig. 2. If the deviation of the particle from one row to the next is a random additive process with possible values $+c$ and $-c$, the normal distribution will be created by the board, which reflects the cumulative additive effects of the sequence of decision points. But if the deviation of the particle from one row to the next is a random multiplicative process with possible values $\cdot c'$ and $/c'$, the log-normal distribution will be generated. Here c and c' are certain constants.[10] (A recent good recapitulation of the theory of Galton board and log-normal distribution can be found in Ref. [11] and thus no details are given in this paper)

The Galton board model inspires us to view the driver's velocity adjusting process as a similar generative model. It is obvious that drivers tend to take very careful acceleration when the spacing between the two vehicles is small and does not want to speed up at once after braking. The deviation of the particle to the left is equivalent to the following vehicle's accelerating action, since the relative speed decreases slowly at this period; while the deviation to the right is equivalent to the following vehicle's braking action, since the relative speed increases quickly at this period. Thus, the tracking errors deviating from the ideal time headways will be accumulated gradually and finally formulate the log-normal type distributions.

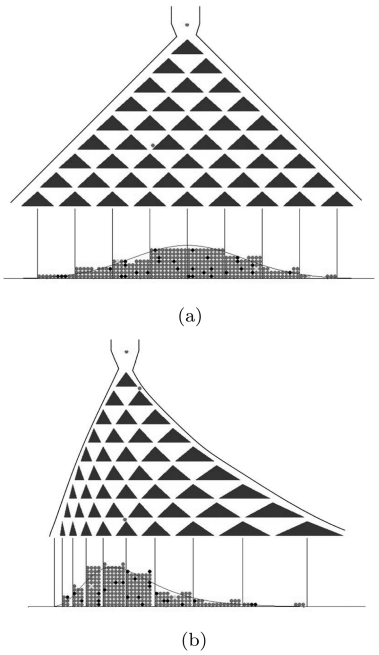


Fig. 2. Diagram of two Galton boards yielding normal (a) and log-normal (b) distributions respectively. If the tip of a triangle is at distance x from the left edge of the board, triangle tips to the right and to the left below it are placed at $x + c$ and $x - c$ for the normal distribution, and $x \cdot c'$ and x/c' for the log-normal, where c and c' are constants.

According to this idea, the variation dynamics of time-headway $t_{\rm h}(t)$ should be depicted by the following equation without losing any generality, if it follows log-normal distribution

$$t_{\rm h}(t) = \begin{cases} \beta t_{\rm h}(t-1), & \text{with probability } (1-p), \\ \dfrac{1}{\beta} t_{\rm h}(t-1), & \text{with probability } p, \end{cases} \tag{3}$$

where β is a positive coefficient, $0 < p < 1$.

If $\beta = 1$, the system will enter the steady state immediately, since every follower will exactly track its leader. However, this contradicts the practices. Here we assume that $0 < \beta \lesssim 1$ together with $0 < p < 0.5$, since drivers tend to keep a close spacing.

More precisely, they can be described as follows. Suppose $v_i(t)$ and $x_i(t)$ are the velocity and head position of the i-th vehicle (follower) at time t, respectively. Similarly, $v_{i-1}(t)$ and $x_{i-1}(t)$ are the velocity and head position of the $(i-1)$-th vehicle (leader) at

time t respectively. The $g_i(t) = x_{i-1}(t) - x_i(t) - l$ denotes the space-gap between the two vehicles at time t, where l denotes the uniform length of the vehicles. The simulation time span is 1 s.

Noticing $t_{\rm h}(t) \approx g_s(t)/v(t+1)$, we have

$$\widetilde{v}_i(t+1) = \begin{cases} \beta v_i(t)\dfrac{g_i(t)}{g_i(t-1)}, & \text{with } p, \\ \dfrac{1}{\beta}v_i(t)\dfrac{g_i(t)}{g_i(t-1)}, & \text{with } (1-p), \end{cases} \tag{4}$$

which has a similar velocity updating formula as the famous GHR type car-following model[12,13]

$$\widetilde{v}_i(t+1) = v_i(t) + cv_i^p(t)\frac{v_{i-1}(t) - v_i(t)}{g_i^q(t)}, \tag{5}$$

where c, p and q are three non-negative exponent coefficients calibrated from practical data.

Obviously, the proposed model and the GHR model propose different formulas to interpret the following intuitive hypothesis: a driver's acceleration was proportional to the vehicle different $v_{i-1}(t) - v_i(t)$ and the deviation from a set following distance $g_i(t)$. However, simulation results show that the GHR model cannot yield log-normal distributions, no matter what parameter set (c, p and q) is chosen.

The above equation determines the key model characterizing the major car-following dynamics of vehicles. However, in order to accurately describe the driving behaviors on highway, we still need to make some modifications.

2.2. The complete model

In this paper, the complete simulation model is assumed to consist of five modes: 1) stopped; 2) starting-up; 3) free-driving; 4) slowing-down and 5) car-following states, see Fig. 3.

At the beginning of each round of simulation, the simulation system will judge the current mode according to the updating rules below. Then, a desired speed $\widetilde{v}_i(t+1)$ would be roughly determined according to the current mode. At the end of each round, the acc/deceleration limits and collision-free constraints would be checked to modify the $\widetilde{v}_i(t+1)$. For simplicity, a symbol flag is introduced here, where flag == 1 means the vehicle is in the starting-up mode, and flag == 0 indicates otherwise.

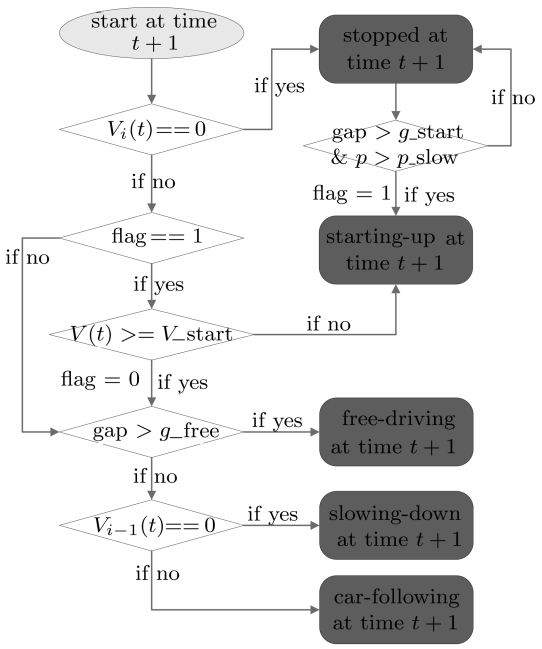


Fig. 3. Flowchart illustrating how to determine the current mode.

(i) Stopped mode

Entering condition: if $v_i(t) = 0$, then the i-th vehicle would enter stopped mode at time $(t+1)$, i.e, $v_i(t+1) = 0$.

Leaving condition: as suggested in Ref. [14], the vehicle will leave the stopped mode and enter the starting-up mode if the two conditions below are both satisfied: a) the space-gap ahead becomes larger than a pre-selected threshold at time t ($g_i(t) > g_{\rm start}$); b) $\gamma > p_{\rm slow}$, where γ is a random number uniformly generated from $[0, 1]$ every round, $p_{\rm slow}$ denotes the pre-selected slow-to-start probability. In this case, flag will be set as flag = 1 and the vehicle will transfer to starting-up mode for further modification. Otherwise, the vehicle will stay in the stopped mode at $(t+1)$.

Similar to the slow-to-start features proposed in Refs. [15] and [16], we assume that $p_{\rm slow}$ increases with the stopping time here as

$$p_{\rm slow} = \begin{cases} p_1 + (p_2 - p_1)\left(\dfrac{t_{\rm stop}}{t_{\rm slow}}\right)^4, & t_{\rm stop} \le t_{\rm slow}, \\ p_2, & t_{\rm stop} > t_{\rm slow}, \end{cases} \tag{6}$$

where $t_{\rm slow}$ is a pre-selected constant. The $t_{\rm stop}$ denotes how many seconds pass once the vehicle enters the stopped condition and will be refreshed to 0 after starting-up.

(ii) Starting-up mode

Entering condition: if flag == 1 , the vehicle will enter the starting-up mode.

Leaving condition: if the velocity becomes larger than a pre-selected threshold, $v_i(t) \geq v_{\rm start}$, the vehicle will leave this mode, and flag will be set as flag = 0.

In this mode, the vehicle would accelerate until $v_{\rm start}$ is reached. The limit of ac/deceleartion will be guaranteed in the following Eq. (12) and thus omitted here.

$$\widetilde{v_i}(t+1) = v_{\rm start}. \tag{7}$$

(iii) Free-driving mode

Entering/leaving condition: Else if and only if the space-gap ahead becomes larger than a pre-selected threshold (the maximum coupling distance) at time t, $g_i(t) > g_{\rm free}$, the vehicle will enter free-driving mode. The maximum coupling distance $g_{\rm free}$ is assumed to be velocity-dependent as

$$g_{\rm free} = \lambda v_i(t) + \theta, \tag{8}$$

where λ and θ are two positive coefficients.

In this mode, the vehicle tends to accelerate to the maximum velocity $v_{\max}$. The limit of ac/deceleartion will be guaranteed in the following Eq. (12) and thus omitted here.

$$\widetilde{v_i}(t+1) = v_{\max}. \tag{9}$$

(iv) Slowing-down mode

Entering/leaving condition: Else if and only if $v_{i-1}(t) = 0$, the i-th vehicle would enter the slowing-down mode.

In this mode, the vehicle tries to approach the leading vehicle until a pre-selected stopped gap $g_{\rm stop}$ is reached. The limit of ac/deceleration will be guaranteed in the following Eq. (12) and thus omitted here.

$$\widetilde{v_i}(t+1) = g_i(t) - g_{\rm stop}. \tag{10}$$

(v) Car-following mode

The car-following mode contains two sub-modes here: a) braking sub-mode and b) normal following sub-mode.

a) Braking sub-mode

Entering/leaving condition: if and only if $v_i(t) - v_{i-1}(t) > [g_i(t) - g_{\rm stop}]/H$ and $v_{i-1}(t) > W$, the i-th vehicle will enter the speed-adaptation braking sub-mode. Here, H and W are two positive coefficients.

In this mode, the driver considers that the velocity is high in comparison with the leading one. He/she tends to keep the same velocity as the leading vehicle and would decelerate (noticing that $v_i(t) > v_{i-1}(t)$ have been guaranteed in this sub-mode)

$$\widetilde{v_i}(t+1) = v_{i-1}(t). \tag{11}$$

b) Normal-following sub-mode

Otherwise, the vehicle is running in the normal following sub-mode depicted by Eq. (4).

Finally, the $\widetilde{v_i}(t+1)$ are checked by considering the acc/deceleration limits as

$$v_i(t+1) = \begin{cases} \min\{v_i(t) + a^+_{\max}, \ \widetilde{v_i}(t+1), \ v_{\max}, \ g_i(t) - g_{\rm stop}\}, & \text{if } \widetilde{v_i}(t+1) \geq v_i(t), \\ \min\{\max\{v_i(t) - a^-_{\max}, \ \widetilde{v_i}(t+1), \ 0\}, \ g_i(t) - g_{\rm stop}\}, & \text{if } \widetilde{v_i}(t+1) < v_i(t), \end{cases} \tag{12}$$

and the position of vehicle is updated as

$$x_i(t+1) = x_i(t) + v_i(t+1). \tag{13}$$

3. Simulations of the proposed model

3.1. Parameter selection

The parameters in this model are divided into two groups: the parameters associating with car-starting/stopping process and the parameters associating with car-following process.

For the first group, we have

i) $v_{\max}$, $g_{\rm start}$ and $g_{\rm stop}$ are chosen according to practical observations and usual settings as $v_{\max} = 27$ m/s, $g_{\rm start} = 2.2$ m, $g_{\rm stop} = 1.5$ m;

ii) $t_{\rm slow}$, p_1 and p_2 are chosen similar to Ref. [16] as $t_{\rm slow} = 10$ s, $p_1 = 0.33$, $p_2 = 0.45$;

iii) λ and θ are chosen similar to Ref. [2] as $\lambda = 2$, $\theta = 3$ m;

iv) The parameter $v_{\rm start}$ is a critical parameter determining when to enter the starting mode from the car-following mode. Its value should be chosen to guarantee that the key model Eq. (4) will not be applied when the speed is low. Based on simulation tests, this parameter is set as $v_{\rm start} = 3$ m/s.

For the second group, we found the following coupling relations among the parameters, see Fig. 4.

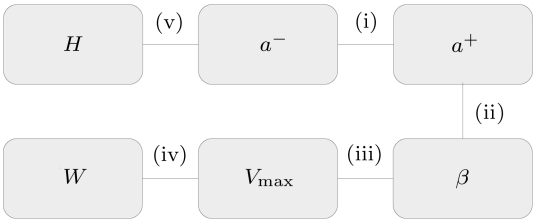


Fig. 4. The coupling relation diagram of the parameters with respect to car-following.

(I) First, $a^+_{\max}$ and $a^-_{\max}$ are determined according to usual settings as $a^+_{\max} = 3$ m/s, $a^-_{\max} = 5$ m/s;

(II) Second, we need to roughly guarantee $a^+_{\max} > (1-\beta)v_{\max}$, if we want the key model Eq. (4) to become the dominant mechanism that shapes the car-following process. Here, we set $\beta = 0.9$ and correspondingly $p = 0.45$;

(III) Third, drivers are less sensitive when the speed is low and thus the parameter W is introduced to simulate this phenomenon. If W is too small, the perturbation in the low velocity section would be too small, leading to the extinction of wide moving jams in simulation. If W is too large, the driving behaviour would be very unstable, which contradicts with observation. Since $v_{\max}$ is set as $v_{\max} = 27$ m/s above, the acceptable value range of W is between 8 and 10. Particularly, we set $W = 9$ m/s;

(IV) Fourth, a larger H would make the deceleration easier to occur, but a too large H would threaten the dominance of the key model Eq. (4). On the other hand, a too small H requires a very large $a^-_{\max}$, which leads to a very severe deceleration of vehicles. Thus, we select H as $H = 5$ s based on simulation tests.

Besides, all the vehicles have the same length as $l = 4$ m.

3.2. Simulation results

Figure 5 shows the corresponding distributions of the simulated time-headways within three different velocity ranges. All the simulated time-headways pass the 95% Kolmogorov–Smirnov (K–S) hypothesis test for log-normal distribution with P-value 0.06, 0.16 and 0.17 respectively. This proves that the new model exactly yields the log-normal type time-headway distribution as observed (comparatively, many previous models yield symmetric distributions, i.e. Fig. 7 of Ref. [17]). As the velocity of the vehicle increases, the mean time-headways of such log-normal type distributions will approach the saturation headway. This fits the observations,[18,19] too.

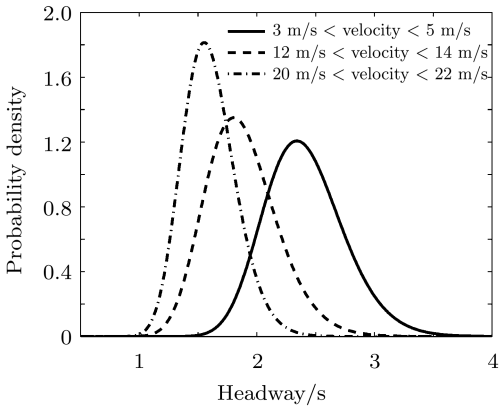


Fig. 5. Estimated log-normal type probability density function for simulated time-headways $t_{\rm h}$ (in seconds).

The macroscopic traffic stream characteristics on a circular single-lane road are also measured according to Ref. [20], where the length of road is 27000 m. Figure 6 shows that the proposed model can correctly reproduce the synchronized flow state. Similar to Ref. [16], hysteresis effect can be clearly found in the diagram given in Fig. 7. This indicates that the proposed model can reproduce the complex behaviour observed in highway systems.

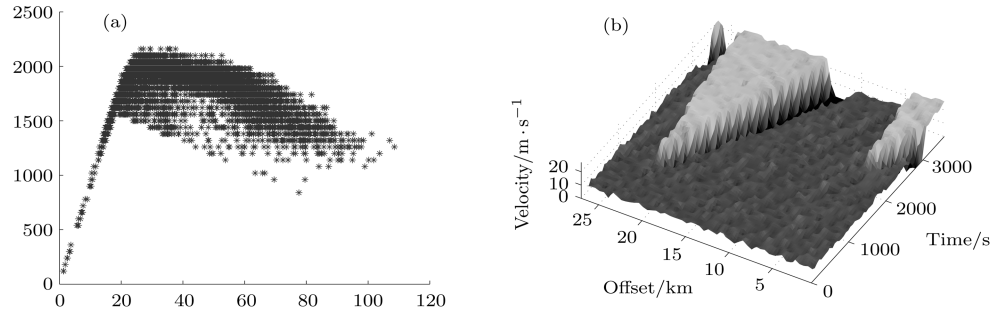


Fig. 6. (a) The (k, q) diagrams for the model during synchronized flow state, obtained by local measurements. (b) The spatial-temporal diagram of the transition from synchronized flow to jams.

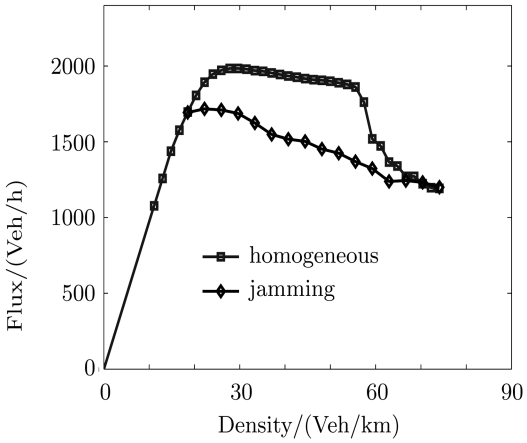


Fig.7. The fundamental diagram of the model, obtained by starting from two initial states: jammed states (low branch) and homogeneous states (upper branch).

4. Conclusion

A new car-following model is designed in this paper to reproduce the observed time-headway distributions as well as the complex traffic phenomena. The research purposes are twofold here:

I) Log-normal distribution is suggested as a useful distribution model to model the vehicle time-headways;

II) Previous physical interpretations focus on the steady-state macroscopic-level statistics of the vehicle time-headways. Differently, this method provides a microscopic-level dynamic explanation, which can also be used to simulate the transient-state statistics of inter-arrival and inter-departure vehicle queuing interactions.

References

[1] Helbing D 2001 *Rev. Mod. Phys.* **73** 1067
[2] Kerner B S 2004 *The Physics of Traffic* (Heidelberg: Springer)
[3] Krbalek M, Seba P and Wagner P 2001 *Phys. Rev.* E **64** 066119
[4] Krbalek M and Helbing D 2004 *Physica* A **333** 370
[5] Abul-Magd A Y 2007 *Phys. Rev.* E **76** 057101
[6] Thiemann C, Treiber M and Kesting A 2008 *Traffic Flow Theory and Characteristics 2008* 90
[7] Piao J and McDonald M 2003 *Proceedings of IEEE Intelligent Vehicles Symposium* 462
[8] Zhang G, Wang Y, Wei H and Chen Y 2007 *Traffic Flow Theory 2007* 141
[9] Galton F 1889 *Natural Inheritance* (London: Mac Millan)
[10] Crow E L and Shimizu K 1988 *Log-normal Distributions: Theory and Applications* (New York: Markel Dekker, Inc.)
[11] Limpert E, Stahel W A and Abbt M 2001 *Bioscience* **51** 341
[12] Gazis D C, Herman R and Potts R B 1959 *Operations Research* **7** 499
[13] Brackstone M and McDonald M 1999 *Transportation Research,* Part F, *Traffic Psychology and Behaviour* **2** 181
[14] Lee H K, Barlovic R, Schreckenberg M and Kim D 2003 *Traffic and Granular Flow 03* 253
[15] Jiang R and Wu Q 2005 *Eur. Phys. J.* B **46** 581
[16] Gao K, Jiang R, Hu S, Wang B and Wu Q 2007 *Phys. Rev.* E **76** 026105
[17] Bando M, Hasebe K, Nakayama A, Shibata A and Sugiyama Y 1995 *Phys. Rev.* E **51** 1035
[18] Kerner B S, Klenov S L, Hiller A and Rehborn H 2006 *Phys. Rev.* E **73** 046107
[19] Schonhof M and Helbing D 2007 *Transp. Sci.* **41** 135
[20] Maerivoet S and De Moor B 2005 *Phys. Rep.* **419** 1